*Proceedings of the 20th International Conference on Soil Mechanics and Geotechnical Engineering– Rahman and Jaksa (Eds)*


# Numerical prediction of the Ballina test embankment using an advanced constitutive model

## Prédiction numérique du remblai d'essai de Ballina utilisant un modèle de comportement avancé

**James Barron**, Mohamed Rouainia & Tom Charlton
*School of Engineering, Newcastle University, United Kingdom, j.r.barron2@newcastle.ac.uk*

ABSTRACT: This paper uses an advanced kinematic hardening constitutive model that accounts for loss of structure to perform a prediction of settlement and excess pore pressures of the Ballina test embankment in a 2D finite element code. The model parameters were derived from advanced laboratory and in situ testing and calibration of the advanced model was performed against undrained triaxial tests. The modelling was guided by recommendations from the Newcastle symposium for the prediction of embankment behaviour on soft soil. The equivalent vertical permeability method was used to model the effect of prefabricated vertical drains (PVDs) underneath the embankment. The results indicated that the constitutive model was able to accurately capture the evolution of surface settlement after initial loading and total settlement after the 1091-day monitoring period. A good prediction of excess pore pressures was achieved, although the model tended to overestimate the developed pore pressures. This was attributed to the predicted failure mechanism in the finite element model and equivalent permeability adopted.

RÉSUMÉ: Dans cet article, un modèle de comportement à écrouissage cinématique pour les sols structurés, est utilisé pour prédire les tassements et les pressions interstitielles excessives du remblai d'essai Ballina par la méthode des éléments finis 2D. Les paramètres du modèle ont été déterminés au moyen d'essais avancés de laboratoire et in situ, et la calibration du modèle avancé a été déduits à partir des résultats d'essais triaxiaux non drainés. Cette modélisation tenait compte des recommandations du symposium de Newcastle pour la prédiction du comportement des remblais construits sur argiles molles et cimentées. La méthode de perméabilité verticale équivalente a été utilisée pour modéliser l'effet des drains verticaux préfabriqués (PVD) installés sous le remblai. Les résultats numériques ont indiqué que le modèle de comportement est capable de capturer l'évolution du tassement de surface après le chargement initial et le tassement total après la période de surveillance de 1091 jours avec précision. La concordance obtenue de la pression interstitielle excessive est bonne, bien qu'il faille remarquer que le modèle a tendance à surestimer les pressions interstitielles développées. Ceci a été attribué au mécanisme de rupture prédit dans le modèle des éléments finis ainsi qu'à la perméabilité équivalente adoptée.

KEYWORDS: Trial embankment; finite element; constitutive modelling; soft soils; prefabricated drains.

## 1 INTRODUCTION

The Ballina soft soil field test facility is a trial embankment founded on soft structured estuarine clay located in Australia's National Field Testing Facility (NFTF), Ballina, New South Wales. It was built to stimulate research with the aim of reducing the cost and risk of infrastructure construction on low-strength, poor-quality onshore and offshore soils. The facility was motivated by the construction of the Ballina Bypass, where settlements of up to 6.5m were recorded and there was a large difference between predicted and observed settlements at a number of embankments (Kelly, 2013; Kelly *et al.*, 2018).

The test embankment was constructed in 2013 and installed with prefabricated vertical drains (PVDs). The site has undergone a comprehensive programme of advanced geotechnical sampling to recover good quality undisturbed samples (Pineda *et al.*, 2014), and advanced laboratory testing to fully characterise the material (Pineda *et al.*, 2016). In addition, two boreholes for in-situ testing were used to identify stratigraphic boundaries and supplement the geotechnical parameters (Kelly *et al.*, 2014; Kelly *et al.*, 2017). The embankment is fully instrumented to monitor dissipation of excess pore pressures, vertical and horizontal deformations, and soil pressure (Pineda *et al.*, 2016; Kelly *et al.*, 2017). Data from the Ballina test embankment site is available for use by the geotechnical community via a web-based application named "Datamap" (Doherty *et al.*, 2018). An embankment prediction symposium held in 2016 (Sloan and Kelly, 2016) attracted twenty-eight predictions using a variety of constitutive models and numerical methods to predict evolution of pore pressures and settlement, only a limited number of which were advanced models that accounted for the destructuration of soft, natural clays.

In this paper, an advanced kinematic hardening constitutive model is used in a 2D finite element (FE) analysis of the Ballina test embankment. The constitutive model accounts for many of the complex mechanisms that govern the behaviour of soft soils under embankment loads, including the loss of natural structure, degradation of initial stiffness and the early onset of plastic strains and generation of excess pore-water pressures. Model parameters were carefully derived from advanced laboratory and in situ testing, with further calibration against the results of undrained triaxial tests. PVDs were modelled using the equivalent vertical permeability method. Results are presented in terms of the predicted settlement and pore-water pressures under the embankment during and after construction and compared with the monitored field values.

## 2 BALLINA TRIAL EMBANKMENT

### 2.1 *Site conditions*

Index and mechanical properties of the soils have been extensively investigated by laboratory testing of high-quality undisturbed samples by Pineda *et al.* (2016). The Ballina clay is characterised by a high natural water content ($w_{nat}$), high void ratio, low density, high plasticity, is lightly overconsolidated and has very low to low undrained strength. The initial void ratio $e_0$ increases with depth from an average value of 2.1 between $z$ = 1.5m and 4m, to $e_0$ = 3.0 between $z$ = 4m and 10.5m. The dry density ($\rho_d$) varies between 1.0t/m$^3$ and 0.8t/m$^3$ to a depth of $z$ = 4m then decreases to between 0.8t/m3 and 0.6t/m3. The particle size distribution indicates a clay content of 60% increasing to 70-80% below $z$ = 6m corresponding to an increase in plasticity limit (PL) and $w_{nat}$.

The preconsolidation stress σ'$_c$, corrected from Pineda *et al.* (2016) by a factor of 0.84 for strain rate effects (Watabe *et al.*, 2012), increases from an average of 50kPa in the upper part of the clay, to 70kPa in the lower part. This indicates a degree of overconsolidation with an average overconsolidation ratio (OCR) of 1.9 from $z$ = 1.5 to 4.0m, 1.6 from $z$ = 4.0 to 6.0m and 1.4 from $z$ = 6 to 10.5m. The undrained shear strength ($s_u$) increases linearly with depth from an average value of 13 kPa at $z$ = 3m to 20-22 kPa at $z$ = 7m. Permeability ($k_w$) values calculated from constant rate of strain (CRS) oedometer tests by Pineda *et al.* (2016) for Ballina clay ranged between 8.64 × $10^{-4}$ and 8.64 × $10^{-7}$m/day with a clear reduction in permeability below $z$ = 4 m.

Based on this data, the following soil layering was proposed:

- Layer 1 (ground level to $z$ = 1.5m) comprising a heterogenous alluvial weathered crust layer formed of sandy clayey silt;
- Layer 2 ($z$ = 1.5 to 4.0m) comprising the upper unit of Ballina clay characterised by increasing plasticity limit (PL), liquid limit (LL), void ratio, $w_{nat}$, clay content, reduced sand and silt content, reduced $\rho_d$ and very low $s_u$;
- Layer 3 ($z$ = 4.0 to 6.0m) comprising the middle unit of Ballina clay characterised by an increase in PL, LL, $w_{nat}$, void ratio, clay content, increase in $s_u$ and reduction in OCR;
- Layer 4 ($z$ = 6.0 to 10.7m) forming the lower Ballina clay unit with the highest PL, LL, $w_{nat}$, void ratio, clay content, increase in $s_u$ and further reduction in OCR;
- Layer 5 ($z$ = 10.7 to 14.0m) comprising a transition zone of clayey silty sand;
- Layer 6 ($z$ = 14.0 to 19.3m) comprising a fine sand.

A cross section of the Ballina test embankment is shown in Figure 1, indicating the soil layers considered in this paper.

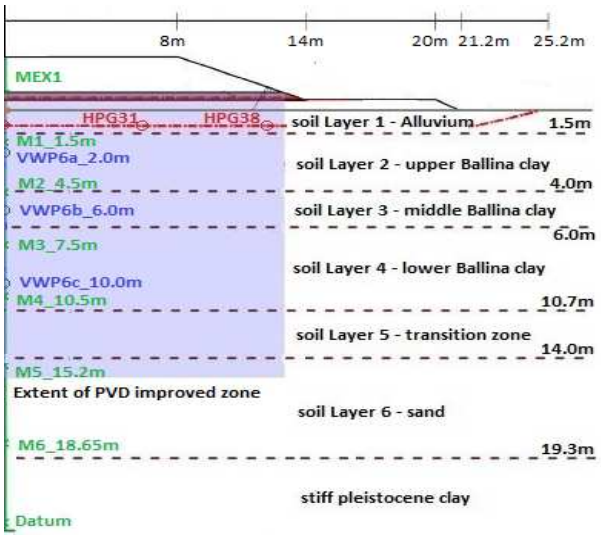


Figure 1. Cross section of Ballina test embankment. Soil layering and location of instrumentation adapted from Kelly *et al.* (2018).

### 2.2 *Geometry and construction sequence*

The embankment is built upon a working platform 95m long × 40m wide × 0.6m thick, constructed with earth fill underlain by a Geofirma AS270c geotextile. The fill material comprises high plasticity Ballina clay sourced from the nearby Ballina Bypass construction. The embankment structure above the working platform is 83m long × 24m wide. The base is formed of a 0.4m thick sand drainage layer separated from the earth fill by a Geotex Propex 801M geofabric. The embankment has been placed in layers above the sand drainage layer and has been constructed to a height of 3m with slopes at a 1.5H:1V ratio.

Prior to embankment construction, monitoring instrumentation was installed extensively in the PVD-improved embankment. This included nine vibrating wire piezometers (VWP) to measure pore pressure (VWP1a/b/c; VWP2a/b/c; VWP6a/b/c), one magnetic extensometer located in the centre of the embankment with eight magnets to measure the vertical displacement of soil at different depths (M0-M6 + datum), one hydrostatic pressure gauge to record settlement continuously across the width of the embankment at a depth of $z$ = 0.9m (HPG1Aa-Ab), four settlement plates placed along the centre line of the embankment to record the settlement of the ground surface (SP1 to SP4) and two inclinometers, Inclo 1 and Inclo 2. The construction profile and selected installed instrumentation is shown in Figure 1.

## 3 CONSTITUTIVE MODEL

### 3.1 *Kinematic hardening model*

The behaviour of the soft Ballina clay is simulated using an advanced constitutive model developed by Rouainia and Muir Wood (2000). The RMW model extends the classic Modified Cam Clay model to include the effects of anisotropy and structure within the framework of kinematic hardening and bounding surface plasticity. The model is also able to describe complex features of realistic soil behaviour including small strain stiffness, stiffness degradation with strain, stress history and non-monotonic loading. The capabilities of the model have been well documented in a number of studies (e.g. González *et al.*, 2012; Panayides *et al.*, 2012; Rouainia *et al.*, 2017; Charlton and Rouainia, 2021) but the model is yet to be benchmarked against a fully characterised and instrumented test embankment founded on soft structured clay installed with PVDs.

### 3.2 *Calibration*

The parameters for the RMW model are easily obtained from standard laboratory tests (triaxial and oedometer) in addition to a stress-strain curve fitting procedure of undrained triaxial tests. The parameters were calibrated separately for Layers 2, 3 and 4 (Ballina clay). The intrinsic properties and the definition of the initial stress state are summarised in Table 1. The modified compression index $\lambda^*$ and the modified swelling index $\kappa^*$ were obtained from CRS oedometer tests in ln (1+$e$): ln $p'$ space, where $p'$ is the mean effective stress. $M$ was obtained from the slope of the critical state line in undrained triaxial tests and the value of Poisson's ratio was assumed to be 0.3.

OCR was determined from CRS tests provided by Pineda *et al.* (2016), where the preconsolidation stress was estimated using the strain energy method (Becker *et al.*, 1987), corrected for strain rate effects as previously described. The lateral earth pressure coefficient $K_0$ was obtained through $K_0$=(1–sin $\varphi'$)OCR$^{\sin \varphi'}$ and the angle of friction at critical state.

The remaining model parameters describe the influence of structure, destructuration, anisotropy and stiffness degradation on the mechanical behaviour of the clay. These were calibrated to obtain a good fit with the stress-strain curves recorded in undrained triaxial tests. The parameters are summarised in Table 2. The RMW simulation of the stress-strain response is illustrated in Figure 2, where the numerical prediction is compared against experimental data from Layer 4.

Table 1. Intrinsic parameters and initial stress state.

| Soil layer | Elastic | | Plastic/ elastic-plastic | | Initial stress state | |
|---|---|---|---|---|---|---|
| | $\kappa^*$ | $\nu$ | $\lambda^*$ | $M$ | $OCR$ | $K_0$ |
| 2 | 0.013 | 0.3 | 0.189 | 1.47 | 2.07 | 0.61 |
| 3 | 0.016 | 0.3 | 0.334 | 1.52 | 1.68 | 0.54 |
| 4 | 0.017 | 0.3 | 0.297 | 1.47 | 1.44 | 0.52 |

Table 2. RMW model parameters.

| Soil layer | Bubble | Destructuration | | Stiffness | | Initial structure | |
|---|---|---|---|---|---|---|---|
| | $R$ | $k$ | $A$ | $\psi$ | $B$ | $r_0$ | $\eta_0$ |
| 2 | 0.8 | 0.8 | 0.75 | 3.6 | 1.7 | 3.8 | 0.4 |
| 3 | 0.67 | 1.4 | 0.75 | 3.6 | 1.7 | 3.8 | 0.4 |
| 4 | 0.56 | 1.9 | 0.75 | 3.6 | 1.4 | 4.0 | 0.4 |

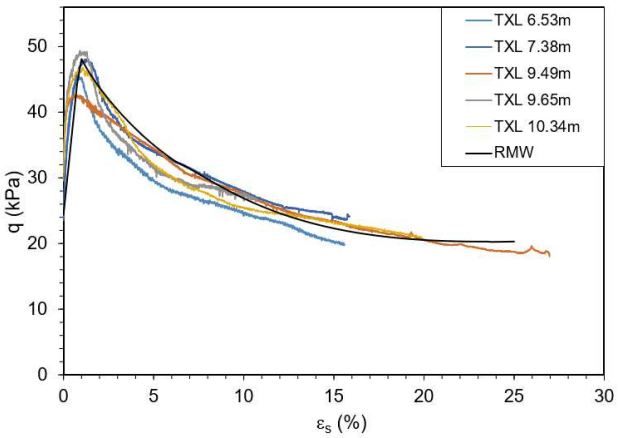


Figure 2. Experimental and numerical undrained triaxial compression tests on Ballina clay (Layer 4).

## 4 FINITE ELEMENT MODEL

### 4.1 *Description*

A 2D plane strain finite element model of the embankment was constructed using PLAXIS 2D 2016 (Plaxis, 2016). Owing to symmetry only half of the embankment was modelled. The mesh is shown in Figure 3 and consisted of 15-noded triangular elements with local refinements in areas where large deformation and high pore pressure gradients were expected. The right-hand boundary of the model was positioned 50m from the centre line of the embankment to avoid any boundary effects. The left and right boundaries were restrained horizontally while the bottom boundary was fixed. Impermeable drainage boundaries were assigned to the lateral and bottom boundaries and the ground surface was allowed to drain freely.

An updated mesh and water pressures were selected to take into account large strains and the effect of fill buoyancy during settlement below a constant phreatic level. The latter effect is important to consider as a settlement of 1.5m could result in a reduction in the applied total stress of around 10kPa, approximately 1/6 of the applied total pressure at the Ballina trial embankment (Kelly *et al.*, 2018).

The phreatic level was set at a constant $z$ = 0.9m to account for the fluctuation observed in the field. The geotextile laid at the ground surface and the geofabric separating the drainage layer from the fill were modelled as geogrids with axial stiffness of 50kN/m.

A coupled deformation and excess pore pressure analysis was performed, meaning that the soil response was determined by the permeability of the material. The sequence of construction adopted in this paper was based upon the time history of filling in the provided Embankment Construction Report (20150708). The embankment was constructed over a period of 63 days whilst the consolidation analysis was performed over 1091 days. This allowed comparison to the field data that was available.

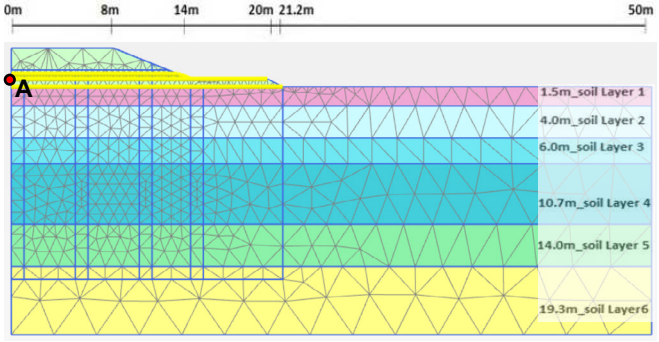


Figure 3. Typical finite element mesh

### 4.2 *Embankment, transition and sand layers*

The embankment, near-surface weathered crust (Layer 1), and transition and sand layers (Layers 5 and 6) were not considered to have a significant effect on the prediction and so were modelled as linear elastic-Mohr Coulomb materials. The parameters are given in Table 3.

Table 3. Parameters for linear elastic- Mohr Coulomb materials.

| Soil layer | $E$ (MPa) | $\nu$ | $c'$ (kPa) | $\varphi'$ (°) | $\psi$ (°) |
|---|---|---|---|---|---|
| 1 | 29.7 | 0.3 | 15 | 38 | 0 |
| 5 | 50.4 | 0.3 | 0 | 38.5 | 8.5 |
| 6 | 71.3 | 0.3 | 0 | 37.6 | 7.6 |
| Embankment fill | 25 | 0.3 | 3 | 38 | 0 |
| Embankment sand | 20 | 0.3 | 0 | 33 | 0 |

### 4.3 *Permeability and PVDs*

The vertical permeability of the soil layers was assigned based on average values calculated in the laboratory from the CRS oedometer tests (Pineda *et al.*, 2016). The permeability was taken at $\sigma'_{yield}$ as representative of the permeability after embankment loading. Due to the limited permeability anisotropy in the Ballina clay deposit (Kelly *et al.*, 2017) the ratio of horizontal to vertical permeability ($k_h/k_v$) was assumed to be 1.1, as suggested by Indraratna *et al.* (2014).

PVDs were modelled using the equivalent permeability method. The installation of PVDs increases the mass permeability of a soil in the vertical direction and the equivalent permeability method assigns a value of vertical permeability which represents the effect of PVD installation on the vertical and radial permeabilities. The equivalent vertical permeability $k_{ve}$ may be calculated based on the formula proposed by Chai *et al.* (2001) as follows:

$$k_{ve} = \left(1 + \frac{2.5l^2}{\mu D_e^2}\frac{k_h}{k_v}\right)k_v \quad (1)$$

where $l$ is the drainage (PVD) length, $k_h$ and $k_v$, are the horizontal and vertical hydraulic conductivity of the natural soil respectively, $D_e$ is the diameter of the unit cell given by: $D_e$ =

1.13$S$ where $S$ is the space between the drains which in this case is 1.2m. The term $\mu$ is given by:

$$\mu = \ln\frac{n}{s} + \frac{k_h}{k_s}\ln s - \frac{3}{4} + \pi\frac{2l^2 k_h}{3q_w} \quad (2)$$

where $n$ is the ratio of the diameter of the unit cell to the diameter of the drain, $n = D_e / D_w$, and $s$ is the ratio of the diameter of the smear zone to the drain diameter (also known as the smear radius ratio), $s = D_s / D_w$, $q_w$ is the discharge capacity of the PVD and $k_s$ is the horizontal hydraulic conductivity of the smeared zone. The equivalent diameter of the drain $D_w$ may be estimated to be 0.454$w$ where $w$ is the drain width (Abuel-Naga *et al.*, 2009) and was assumed to be 0.14m taking into account the disturbance effect of the installation mandrel (Kelly *et al.*, 2018). Based on work carried out at the Ballina test embankment by Indraratna *et al.* (2014) the smear radius ratio at the test site has been estimated to be 7.8, and the ratio of natural to smeared horizontal permeability ($k_h / k_s$) estimated to be 2. The discharge capacity of the PVD was assumed to be $q_w = 100\text{m}^3$/year which is considered a reasonable estimate for preliminary design (Chai *et al.*, 2001). As the PVDs penetrate into the sand layer a condition of two-way drainage exists and $l = H/2$ where $H$ is the thickness of the PVD improved zone (15m).

An equivalent horizontal permeability $k_{he}$ was also assigned to the surrounding drain-improved soil based on the formula originally proposed by Hird *et al.* (1992) as follows:

$$\frac{k_{he}}{k_h} = \frac{D_e^2}{6R_{iz}^2\left[\ln\frac{D_e}{D_s} + \frac{k_h}{k_s}\ln\frac{D_s}{D_w} - 0.75\right]}w \quad (3)$$

where $R_{iz}$ is the radius of influence zone around the vertical drain and for a square pattern $R_{iz} = 0.564S$.

The equivalent vertical and horizontal permeabilities were calculated for Layers 1, 2, 3 and 4 (the upper alluvial crust and Ballina clay) whilst permeability change index $C_k$ values from 0.5 (Layer 1 and 2) to 1.125 (Layer 3 and 4) were adopted based on those reported by Pineda *et al.* (2016). In addition, owing to the clay content of the transition layer (Layer 5), values of $k_{ve}$ and $k_{he}$ reported by Rezania *et al.* (2018) were adopted for this layer.

The coefficient of permeability values used in the model are given in Table 4.

Table 4. Coefficients of permeability.

| Soil layer | $k_v$ | $k_h$ | $k_{ve}$ | $k_{he}$ |
|---|---|---|---|---|
| | *(m/day)* | | | |
| Fill/ sand | $4.75 \times 10^{-2}$ | $4.75 \times 10^{-2}$ | - | - |
| 1 | $1.53 \times 10^{-3}$ | $1.68 \times 10^{-3}$ | $3.08 \times 10^{-2}$ | $3.67 \times 10^{-5}$ |
| 2 | $2.35 \times 10^{-3}$ | $2.59 \times 10^{-3}$ | $4.74 \times 10^{-2}$ | $5.65 \times 10^{-5}$ |
| 3 | $1.15 \times 10^{-4}$ | $1.26 \times 10^{-4}$ | $2.31 \times 10^{-3}$ | $2.75 \times 10^{-6}$ |
| 4 | $8.74 \times 10^{-5}$ | $9.61 \times 10^{-5}$ | $1.76 \times 10^{-3}$ | $2.1 \times 10^{-6}$ |
| 5 | $4.75 \times 10^{-2}$ | $4.75 \times 10^{-2}$ | $5.84 \times 10^{-2}$ | $8.61 \times 10^{-4}$ |
| 6 | 0.862 | 0.862 | - | - |

## 5 RESULTS AND DISCUSSION

The settlement at ground level underneath the centre of the embankment, labelled point A in Figure 2, was selected to compare the numerical prediction against data from settlement plate 2 (SP2) at the same location. The comparison was made over the 1091-day period post-onset of working platform construction that field data were available. The results are shown in Figure 4. An excellent agreement is observed: the simulations predicted an overall settlement of 1.518m in comparison to the observed settlement at SP2 of 1.52m. The FE model was able to accurately capture both the evolution of settlement after initial loading, total settlement at point A after the 1091-day period, and also captures the continuing rate of settlement observed at the end of the monitoring record.

Numerical predictions were also compared with field data from extensometer magnets located underneath the centre of the embankment at depths of 1.5m (magnet M1), 4.5m (M2), 7.5m (M3) and 10.5m (M4), as shown in Figure 5. A good agreement was achieved in general, although the prediction tends to be more accurate at shallower depths. In the deepest magnet within the Ballina clay (M4, $z$ = 10.5m) very small settlements were recorded (0.01m), highlighting the difficulty of accurately predicting small strains at depth.

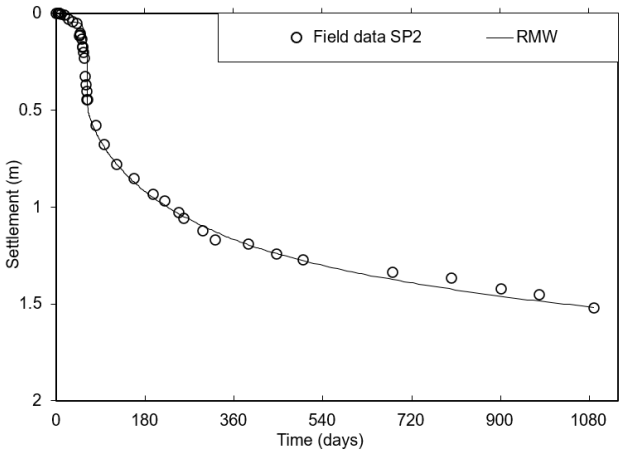

Figure 4. Settlement underneath centre of embankment (point A).

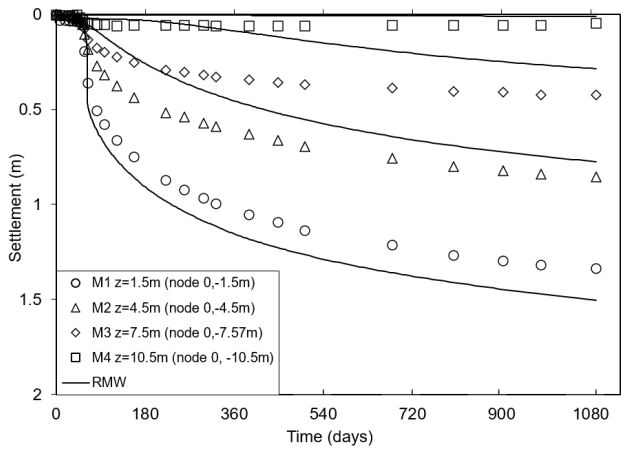

Figure 5. Settlement predictions and field data (magnetic extensometers) at z = 1.5m, 4.5m, 7.5m and 10.5m.

The ability of the FE model to predict excess pore pressures ($P_{excess}$) was assessed by comparing against the VWP data. Following the approach of Kelly *et al*. (2018), to allow for a direct comparison of the numerical excess pore pressures and the VWPs, the uncorrected $P_{excess}$ was corrected to account for changes in hydrostatic pressure caused by VWP settlement and fluctuation in groundwater elevation over time (the site is known to have been flooded after 200 days due to blocking of the drainage system).

The predictions of excess pore pressure underneath the centre of the embankment at z = 2.0m and 10.0m are compared with VWP data from these locations in Figure 6. Again, the numerical model matches well with the field data, successfully capturing

the general development of excess pore pressures at both depths. A spike in initial $P_{excess}$ was predicted by the FE model at VWP6a_($z$ = 2.0m) after around 60 days, shown in Figure 6(a). This is likely to be related to the development of a shear plane predicted by the FE model propagating from underneath the centre of the embankment, as evident in Figure 7. The maximum $P_{excess}$ of 35kPa was greater than the maximum value recorded in the field, and the subsequent rate of dissipation was underestimated. At this shallow depth, features such as near surface fissuring and sandy lenses that would retard peak $P_{excess}$ and encourage the rate of dissipation are not captured in the numerical model. Furthermore, the equivalent permeability method adopted accounts for the smear zone where large $P_{excess}$ concentrations and gradients are expected close to the PVD by averaging over the whole layer. As such the numerical model may overpredict $P_{excess}$ in the centre between the drainage elements.

At $z$ = 10m, a better prediction of the maximum $P_{excess}$ and subsequent dissipation was achieved, as illustrated in Figure 6(b).

(a)

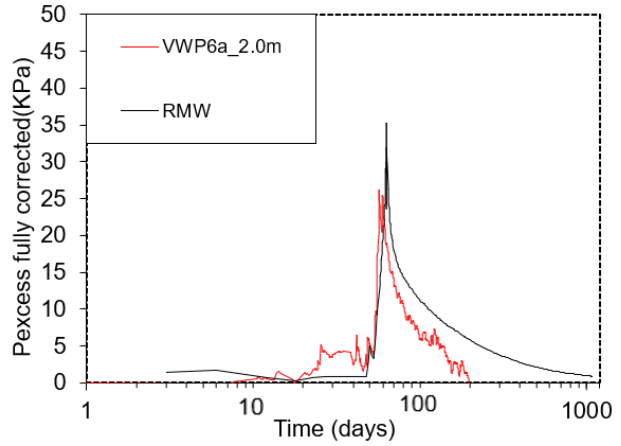


(b)

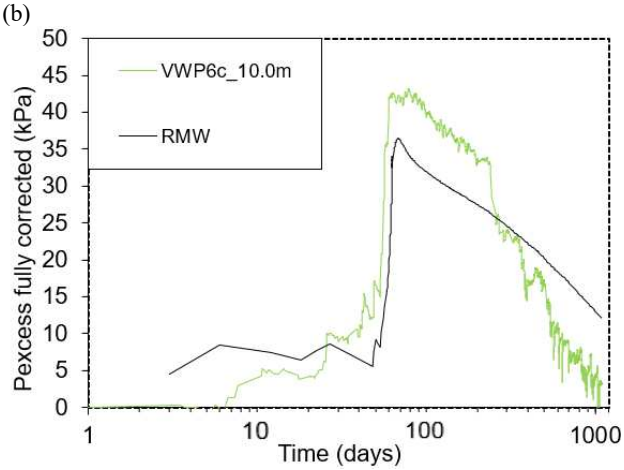


Figure 6. Excess pore pressures ($P_{excess}$) at (a) VWP6a ($z$ = 2.0m) and (b) VWP6c ($z$ = 10.0m).

## 6 CONCLUSIONS

In this paper, an advanced critical state constitutive model formulated in the framework of kinematic hardening was used to predict the settlement and excess pore pressures underneath the Ballina test embankment over a monitoring period of 1091 days. The RMW model was calibrated using a range of high-quality laboratory and in-situ tests, while the modelling was guided by recommendations from the recent symposium for the prediction of embankment behavior on soft soil (Kelly *et al.*, 2018). The FE model of the embankment incorporated PVDs by the equivalent permeability method. In general, a very good agreement was observed between the FE results and field data.

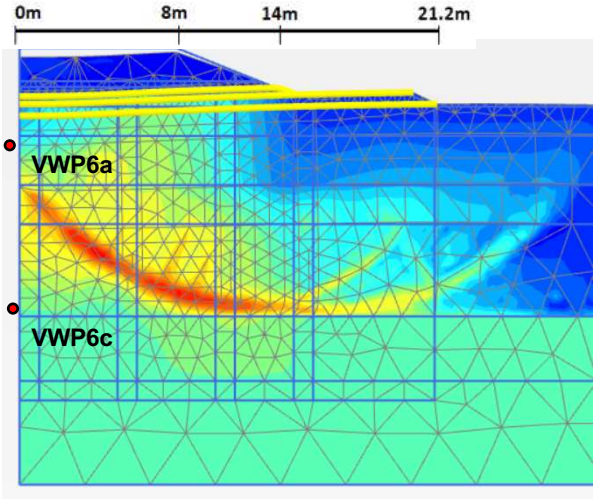


Figure 7. Excess pore pressures underneath the embankment after 63 days. Red = high $P_{excess}$; blue = low $P_{excess}$.

The main findings of this study include:

- The constitutive model was able to accurately predict the evolution of settlement at ground surface underneath the centre of the embankment after initial loading and after the 1091 day monitoring period.
- The settlement profile at depth proved more challenging to predict, highlighting the difficulty of accurately simulating small strain behaviour at depth.
- The FE model matched well with measured excess pore pressures, successfully capturing the general development of excess pore pressures near surface and at depth. The rate of dissipation in the model suggested the permeability parameters were representative.

The study demonstrates that the complex features of realistic soil behavior observed within an embankment founded on PVD-improved soft clay can be captured using an appropriately advanced constitutive model. Further benchmarking of the RMW model and comparison to behavior of the Ballina test embankment is an area of ongoing work by the authors.

## 3 ACKNOWLEDGEMENTS

The first author is supported by an EPSRC CASE studentship with Ryder Geotechnical. This funding is gratefully received and acknowledged.

## 4 REFERENCES

Abuel-Naga H. and Bouazza, A. 2009. Equivalent diameter of a prefabricated vertical drain. *Geotextiles and Geomembranes*, 27(3), 227–31.

Becker, D. E., Crooks, J. H. A., Been, K. and Jefferies, M. G. 1987. Work as a criterion for determining in situ and yield stresses in clays. *Canadian Geotechnical Journal.* 24, No. 4, 549–564.

Chai J-C, Shen S-L., Miura, N. and Bergado, D.T. 2001. Simple method of modelling PVD improved subsoil. *Journal of Geotechnical and Geoenvironmental Engineering*, 127(11), 965–72.

Charlton, T.S. and Rouainia, M. 2021. Cyclic performance of a monopile in spatially variable clay using an advanced constitutive model. *Soil Dynamics and Earthquake Engineering*, 140, 106437.

Doherty, J.P., Gourvenec, S., Gaone, F., Pineda, J., Kelly, R., O'Loughlin,

C.D., Cassidy, M. J., and Sloan, S.W. 2017. A novel web-based application for storing, managing and sharing geotechnical data illustrated using the National Soft Soil Field Testing Facility in Ballina, Australia. *Computers and Geotechnics,* 93, 3–8.

Gonzàlez, N.A., Rouainia, M., Arroyo, M. and Gens, A. 2012. Analysis of tunnel excavation in London Clay incorporating soil structure. *Géotechnique*, 62(12), 1095-1109.

Hird, C. C., Pyrah, I. C. and Russell, D. 1992. Finite element modelling of vertical drains beneath embankment on soft ground. *Geotechnique*, 42(3), 499-511

Indraratna, B., Perera, D. and Rujikiatkamjorn, C. and Kelly, R. 2014. Soil disturbance analysis due to vertical drain installation. *Proceedings of the Institution of Civil Engineers*, *Geotechnical Engineering,* 168, 236–46.

Kelly, R. 2013. Australia's first national facility for soft soils testing. *Civil Engineers Australia*. June, 76-78.

Kelly, R., O'Loughlin, C.D., Bates, L., Gourvenec, S.M., Colreavy, C., White, D.J., Gaone, F.M., Doherty, J.P. and Randolph, M.F. 2014. In situ testing at the national soft soil field testing facility, Ballina, New South Wales. *Australian Geomechanics*, 49(4), December 15-28.

Kelly, R.B, Sloan, S.W., Pineda, J.A., Kouretzis, G. and Huang, J. 2018. Outcomes of the Newcastle symposium for the prediction of embankment behaviour on soft soil. *Computers and Geotechnics,* 93, 9–41.

Kelly, R.B., Pineda, J.A., Bates, L., Suwal, L.P., and Fitzallen, A. 2017. Site characterisation for the Ballina field testing facility. *Géotechnique*, 67(4), 279–300.

Panayides, S., Rouainia, M. and Muir Wood, D. 2012. Influence of degradation of structure on the behaviour of a full-scale embankment. *Canadian Geotechnical Journal*, 49(3), 344-356.

Pineda, J.A., Suwal, L.P., Kelly, R. B. 2014. Sampling and testing of Ballina clay. *Australian Geomechanics*, 49(4), December, 29-40.

Pineda, J.A., Suwal, L.P., Kelly, R. B., Bates, L. and Sloan, S.W. 2016. Characterisation of Ballina clay. *Géotechnique*, 66(7), 556–577.

Plaxis (2016) *PLAXIS 2D 2016 - Reference Manual*. Delft, Netherlands: Plaxis bv.

Rezania, M., Nguyen, H., Zanganeh, H. and Taiebat, M. 2018. Numerical analysis of Ballina test embankment on a soft structured clay foundation. *Computers and Geotechnics*, 93, 61–74.

Rouainia, M. and Muir Wood, D. 2000. A kinematic hardening constitutive model for natural clays with loss of structure. *Géotechnique*, 50(2), 152-164.

Rouainia, M., Elia, G., Panayides, S. and Scott, P. 2017. Nonlinear Finite-Element Prediction of the Performance of a Deep Excavation in Boston Blue Clay. *Journal of Geotechnical and Geoenvironmental Engineering*, 143(5), 04017005.

Sloan, S.W. and Kelly, R.B. 2016. *Embankment and Footing Prediction Symposium*. ARC Centre of Excellence for Geotechnical Science & Engineering, 12-13 September, Fort Scratchley, Newcastle, Australia. ISBN 978-0-9953750-0-0.

Watabe, Y., Udaka, K., Nakatani, Y. and Leroueil, S. 2012. Long-term consolidation behaviour interpreted with isotache concept for worldwide clays. *Soils and Foundations*. 52(3), 449–464.